

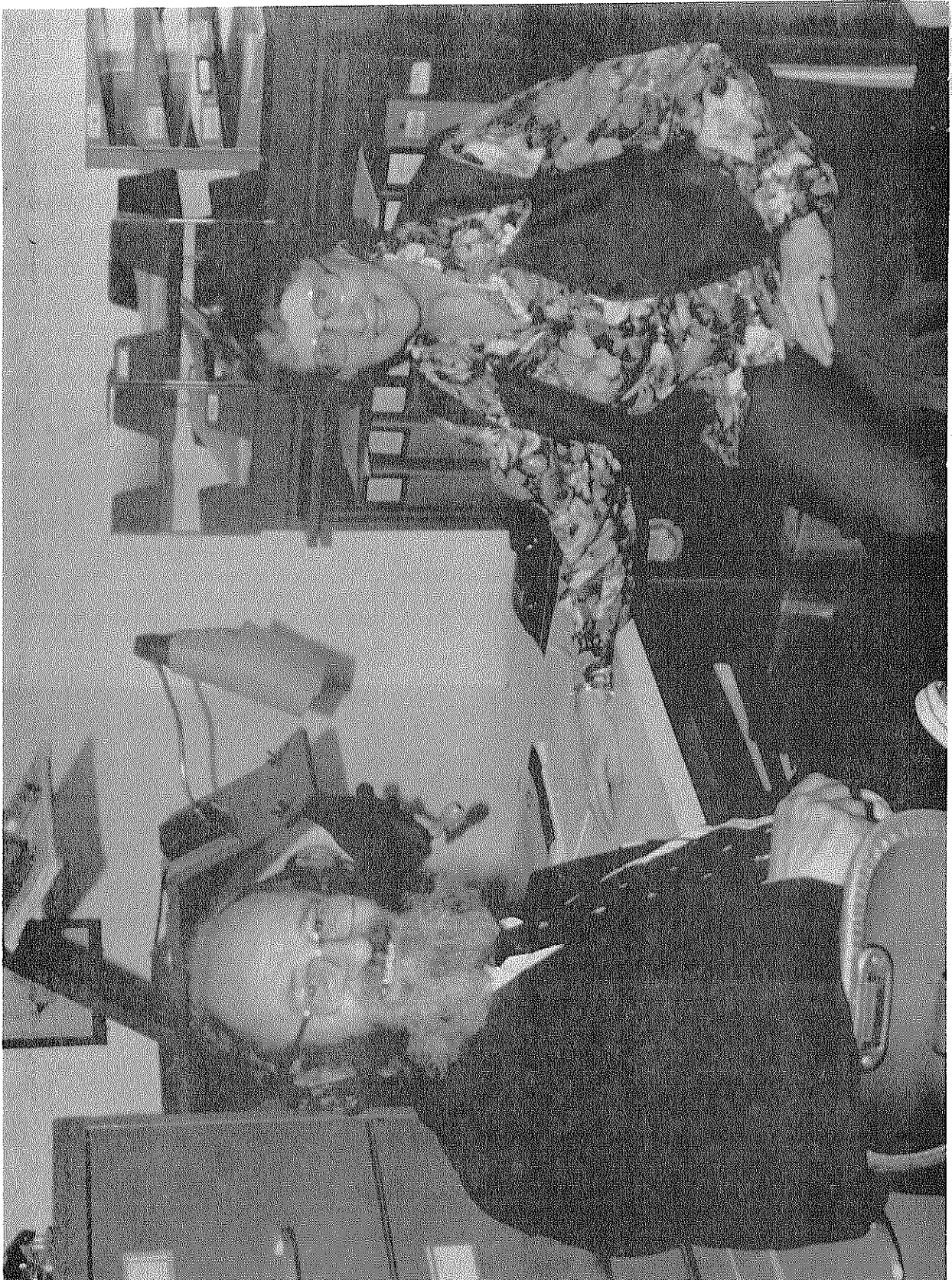
IONOSPHERIC NETWORK ADVISORY GROUP (INAG)*
Ionosphere Station Information Bulletin No. 30**

	<i>Page</i>
I. Introduction	3
II. Solar-Geophysical Data Sets	3
III. INAG Meeting, Australia, December 1979	4
IV. The International Solar- Terrestrial Predictions Workshop	4
V. The Measurement of Ionospheric Absorption	4
VI. The Earth's Field in the Northern and Southern Hemispheres	5
VII. New Layout of Monthly Sheets of Provisional Kn, Ks, Km, and am Indices	8
VIII. Uncle Roy's Column	8
IX. Training Aids	11
X. Correspondence Course	12
XI. Electron Density-Height Problems	13
XII. Index to NOAA's "Solar-Geophysical Data"	15
XIII. Notes on Indexes for UAG-23 and UAG-23A	19

* Under the auspices of Commission G Working Group G.1 of the International Union of Radio Science (URSI).

** Issued on behalf of INAG by World Data Center A for Solar-Terrestrial Physics, National Oceanic and Atmospheric Administration, Boulder, Colorado 80303, U.S.A. The Bulletin is distributed to stations by the same channels (but in the reverse direction) as their data ultimately flow to WDC-A. Others wishing to be on the distribution list should notify WDC-A.





INAG Chairperson W.R. Figgott and Vice Chairperson J. Virginia Lincoln.

I. Introduction

by

W.R. Piggott, Chairman

INAG Bulletin No. 29 was exceptionally large, roughly equivalent to two normal Bulletins. I feel, therefore, that it is not necessary to apologize for this Bulletin being small and lacking some of our standard features--it was prepared hurriedly during my recent visit to WDC-A for STP, Boulder.

As some of you already know, I shall be retiring from my post as Head of the Division of Atmospheric Sciences on December 31, 1979, and shall then have more time for INAG affairs. I am intending to remain active, first completing some unfinished papers, if possible starting some new research using existing data or joining a research organization part-time, and finally I hope it will prove possible for me to visit at least some of your organizations and to discuss your problems with you. In the meantime the remaining INAG Bulletins this year will probably be issued rather irregularly as and when I have the opportunity to work on them.

Past experience has shown that it takes at least a year for even active groups to decide to collaborate in an INAG publication and to prepare ionograms for it. If there are to be ionograms available for me to consider when I have retired, it is important that you start collecting them now. The amount of time that I shall set aside for INAG problems will depend on your response. I probably shall not have personal secretarial facilities, so my output will depend on your input. I understand that WDC-A for STP will be willing to help in the very generous way that they have in the past.

This Bulletin is being prepared at the end of a very successful "International Solar-Terrestrial Predictions Workshop," April 23-27, 1979. I hope to be able to publish more on this when the official report is available. From your point of view one of the more important results is the clearly renewed international and national interest in the practical applications of your data as well as increased scientific interest in it. I attended one of the 14 working groups, one involved in D region prediction and the short article in this Bulletin on absorption is intended to help you understand the background needs for more synoptic study. I also saw direct comparisons between the Australian type IPS 42 ionosonde and a modified C2 ionosonde operated by NOAA, and between the ionogram mode by an Advanced Ionospheric Sounder (HP Radar) and the modified C2 in each case using the same antenna arrays. A short note on the impression these made on me is included but it must be remembered that a short test has only limited value and INAG does not have the facilities to make fair comparisons between commercial equipments.

As the IUGG meeting in Australia overlaps the period when I have to hand over the Division to my successor, it will not be possible for me to attend the very important INAG session to be held in conjunction with that meeting. I hope that all who can will attend and that those who cannot will brief a delegate so that your views and problems can be considered. This will be the first opportunity for most of you to comment on the reports published in INAG 29, p. 3-10. Many points raised there are controversial. What are your views? The response to this meeting will largely guide my next actions on INAG problems. If you feel that I have helped you effectively, try to help me so that this work can continue in the future.

II. Solar-Geophysical Data Sets

Long synoptic solar-geophysical data sets often bear the mark of a single individual who has struggled, through the years, to maintain the continuity, consistency, and quality of the data set. Examples of such data sets in current use are:

1. The Zurich sunspot numbers created first by Wolf and, more recently, maintained by Waldmeier (since 1818);
2. The McMath calcium plage regions compiled by Dodson-Prince (since 1942);
3. The Ottawa 10.7-cm solar radio flux measurements conducted by Covington (since 1947); and
4. The Km, Ks, Kn, and aa-indices of geomagnetic activity since 1957 created and maintained by Mayaud.

These synoptic data sets are of great value because of their continuity, consistency, and quality. The sets have been used extensively and are available to the research community because responsible individuals championed them. Those involved were highly dedicated and determined to continue and maintain their data sets, often against great odds. All of the people listed above have now retired or are about to retire. Readers of the INAG Bulletin who attend international meetings may wish to draw attention to the need to continue some or all of these indices and for suitable action to be taken to maintain their accuracy in the future. I feel that you would wish me to thank these individuals on behalf of the INAG users and have, therefore, written to them on your behalf.

III. INAG Meeting, Australia, December 1979

As stated in INAG 27, p. 15 and INAG 29, p. 25, we intend to hold an INAG meeting in Australia in association with the IAGA General Assembly, Canberra, December 2-15, 1979. No arrangements have been finalized as yet, but information will be given as soon as possible. Please send further items for the provisional Agenda to Dr. D. Cole, Ionospheric Prediction Service, Sydney, Australia.

Agenda

1. Chairman's Introduction.
2. Discussion on Helsinki Report.
3. Actions needed on 'Needs for Ionosondes in the 1980's.'
4. Action on proposed new stations and closure of existing stations.
5. Training problems. Use of Handbooks.
6. Equatorial station networks problems.
7. Changes in parameters, letter symbols, and programs.
8. Status of network.
9. Status of new ionosondes.
10. High-Latitude Working Group.
11. International Digital Ionosonde Group.
12. Discussion of Australia's training and interpretation problems.

At Helsinki some participants regretted that a preliminary meeting had not been arranged for detailed discussion of VI problems before the Assembly. Do those proposing to attend Canberra wish for such a meeting either instead of, or as well as, a meeting during the Assembly? If you have ionograms for the chairman, please bring them to this meeting.

IV. The International Solar-Terrestrial Prediction Workshop

An International Solar-Terrestrial Prediction Workshop was held in Boulder, CO, USA, April 23-27, 1979, under the local auspices of NOAA, to consider how the practical difficulties due to solar and terrestrial phenomena could be minimized. There was much discussion on how periods of disruption in communications, error in navigational systems, interruptions of power line operation, periods of damage to space craft, etc., could be predicted and their effects minimized. Thus both scientists and engineers were involved. Preparatory work had been carried out over the last year by hundreds of collaborators, and 176 participants from 16 countries took part in the Workshop. Reports from the 14 Working Groups were prepared and will be published together with invited reviews and a large number of supporting papers. Results and recommendations of interest to the VI community will be briefly reviewed in an INAG Bulletin when the final texts become available. As there were usually between 5 and 10 sessions active at the same time, it was impossible for any one person to obtain an overall view of the work done.

The size of the support for the work of the Workshop, both before and during the meeting, shows the strength of the renewed interest in solar-terrestrial relations and, in particular to INAG, in the techniques that can be used to monitor the properties of the ionosphere and in the data they produced. There was support for the VI network and attention was drawn to a number of gaps in present knowledge. In his personal capacity, Dr. Piggott, who was active in the D region Working Group, was impressed by the need for more VI stations to attempt to measure absorption both for practical and scientific purposes (see p. 4 this Bulletin).

V. The Measurements of Ionospheric Absorption

The D region, at heights between about 50 km and 95 km, is remarkably difficult to monitor quantitatively. The D region is, however, very important for practical problems, and is scientifically a very complex and interesting zone.

There are two types of practical application:

(i) ELF, VLF, and LF communications and navigational aids are mainly reflected in the lower part of the D region; (ii) the power needed for MF, HF, and VHF applications depends on the absorption likely to be encountered when the signals penetrate the region. In practice it is often more informative and easier to monitor for application (i) using VHF soundings, for example the riometer, or HF methods, for example, D region partial reflection or wave interaction techniques than to use the actual signals. Although the importance of application (i) is obviously very great, the data base available is quite inadequate. This is largely because the techniques have, in the past, been rather difficult, labor intensive, and physical interpretation of the data has been doubtful. Recent developments have changed this and the problems of getting useful data and interpreting them are now greatly reduced. In particular, it now appears practical to develop cheap pulse absorption equipment (method A1) to help solve this problem.

The object of this note is to draw the attention of those administering VI stations, university groups, and research establishments to the value of putting some effort on these problems. The need for action is very great.

Ionospheric absorption provides economical ways of measuring and monitoring changes in the D region of the ionosphere. Actually, the quantity which is measured is $\int N \nu dh$, where N is the electron density and ν the effective electron collision frequency, weighted by a frequency sensitive function that depends on the relative magnitude of the collision frequency and sounding frequency. In practice, measurements made between 1 and 5 MHz are mainly determined by $\int N \nu dh$ in the upper D region, typically above about 85 km and in the E layer. In contrast, data obtained by riometers on frequencies of the order of 30 MHz mainly refer to lower levels. Both techniques tend to be inaccurate and inefficient for monitoring phenomena in their insensitive height ranges, i.e., at low heights for MF, high heights for VHF.

The table below shows some of the corresponding values that could occur so as to illustrate this point.

	FREQUENCY	NORMAL		SID	NORMAL	PCA	ELECTRONS
		NOON	EVENING	(FLARES)		HARD PARTICLES	
MF	2.0 MHz	40db	10db	400db	500db	7db	100db
VHF	30.0 MHz	0.4db	0.1db	4db	8db	6db	1db
Case		a	b		c	d	e

In practice, of course, there are independent changes at widely separated levels, and in particular, there is usually little direct correlation between changes in the upper and lower D region other than those due to the solar zenith angle.

In case (a) absorption can be readily monitored at MF, but demands a very high standard to be measured effectively at VHF. In cases (b), (c), and (e) total absorption at MF and lower HF signals is usual, so the events can be detected but not measured. VHF is most effective for these cases. For case (d) it is very difficult to get adequate accuracy at MF but easy at VHF.

Where both can be used the MF/HF techniques are in general much more sensitive to small absorption than the VHF. Thus, there is a major need to measure both with riometers in the VHF band and by other means in the MF and lower HF bands. Actually there is a fairly good riometer network in existence but the number of stations on the other hand has always been quite inadequate. This is one reason why, despite their weaknesses, stations are encouraged to measure f_{min} or f_{m2} ; at the least it sometimes identifies areas where similar phenomena occur.

At present many groups throughout the world are preparing to take part in the Middle Atmosphere Program which is largely concerned with phenomena in the D-region and its dependence on phenomena at other heights. Many of the phenomena to be studied occur in both parts of the D region, e.g., storm after effects, winter absorption anomalies both regular and event. At low latitudes there is need to establish the reality and magnitude of the equatorial absorption anomaly. On the practical side, CCIR is developing systems of predicting field strengths that depend greatly on the absorption in the upper part of the D region--the part with the least quantitative data.

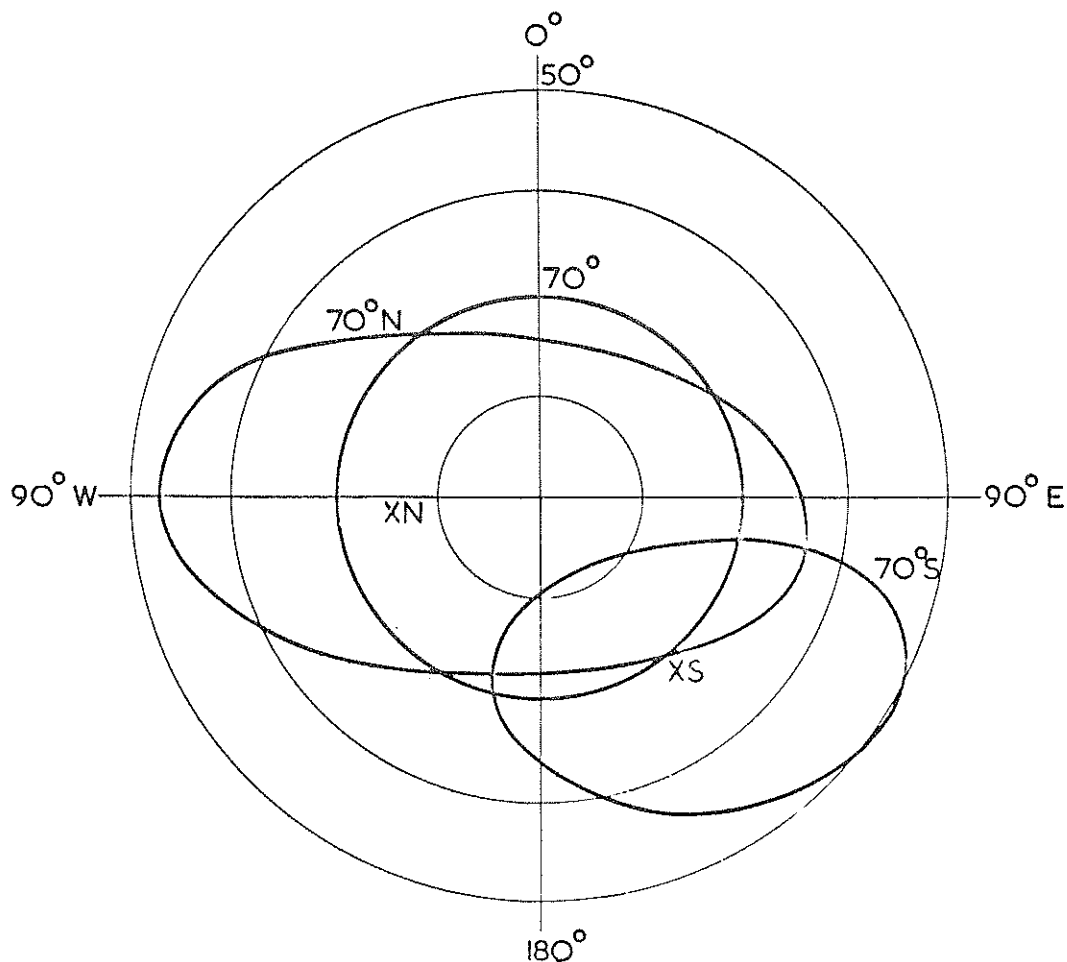
If it can be shown that there would be enough interest in using new AI pulse absorption it is likely, as in the case of the Australian 4A and 4B ionosondes that suitable equipment could be made commercially. At present there is an obvious scientific and practical requirement, but it is not clear that sufficient administrations would be interested to justify the development work necessary.

As with ionosondes, the cost will largely depend on whether the development is subsidized by a government organization and the size of the prospective market. As was shown in the IGY and IQSY, useful data can be obtained using one frequency, but there are times when this will be near a critical frequency and thus misleading. Many stations used two frequencies to reduce these gaps but the minimum ideal is probably four frequencies. If kept simple, the equipments are only slightly more complicated than riometers. Preliminary estimates suggest that 2500 \$ USA, 4000 \$ USA, and 10,000 \$ USA or less should be achievable but no detailed cost studies have been made. If you feel that you might be willing to buy and deploy equipment, please inform the chairman.

VI. The Earth's Field in the Northern and Southern Hemispheres

This short note is intended to draw attention to some of the wide differences in the magnetic configurations in the Northern and Southern Hemispheres. These greatly affect the behavior of the

ionosphere. If this note is found to be interesting to the readers of the Bulletin, I will provide further short notes on other magnetic anomalies and on their influence on the ionosphere. The intention is to keep these simple stressing only the major points. In general in the ionosphere, mechanical forces act primarily along the lines of magnetic field, and electric forces act perpendicular to them. Thus, if the angle of dip is θ , the effect of the acceleration due to gravity on the F layer ionization is $g \sin \theta$ instead of g and acts along the field line, not toward the center of the Earth. Thus, the effects of dynamic forces acting on the F layer tend to be similar along lines of constant magnetic latitude. Fig. A shows the positions of the dip poles in the Northern and Southern Hemispheres as seen on a polar projection where the geographical poles are at the center. Magnetic dip and geographic latitudes of 70° are shown by the thick lines. Actually the internal field is similar to that of a transpolar magnet with a point pole in the south, line pole in the north, and with the magnet displaced from the center of the Earth so that the asymmetry is much greater in the South. Clearly, it is possible to get a much greater range of dip at constant geographic latitude in



Magnetic Latitudes N and S

Figure A. Positions of the north and south dip poles relative to the geographic poles.

the South than in the North at a given geographic latitude and thus to alter the effects of dynamic forces by a greater factor. This is shown more clearly in Fig. B, which gives the lines of constant magnetic latitude (lines where the dip of the field is constant) at 10° intervals and also all past and operational vertical sounding stations. Port Stanley at 51.5° S-- the same latitude as London, England--is tropical in dip coordinates!

The precipitation of particles, magnetospheric boundaries, and interactions between the ionosphere and magnetosphere map down into the ionosphere fairly closely with invariant (or corrected geomagnetic latitude), curves where a constant L shell i.e., constant height above the equator, maps down into the ionosphere. The invariant latitude shown in Fig. C is similar to dip but not so extreme. In the North differences between dip and invariant latitude are relatively small but, as can be seen by comparing Figs. B and C, in the South they are great. Thus, the particles are precipitated along curves which

INAG-30

cross the lines of constant dip, modulating the effects of electric fields accordingly. Also the precipitation zone in the Antarctic Peninsula zone of the Southern Hemisphere occurs at much higher geographic latitudes than are found in the North (and of course at much lower geographic latitudes in the opposite sector that contains the magnetic dip pole).

If you would like this series to be continued, please let us know. There was no response to my first article on the history of the ionosphere letters, INAG 24, p. 2-6, and I have therefore not felt it worthwhile to finish it. You can raise your views verbally at the INAG meeting in Australia or any other INAG meeting if you prefer not to write.

VII. New Layout of Monthly Sheets of Provisional Kn, Ks, Km, and am Indices

In accord with a request by the Working Group on Geophysical Indices at the IAGA Scientific Assembly at Seattle, the monthly sheets of provisional indices Kn, Ks, Km, and am will, in the future, be circulated as direct electrostatic copies of the computer listing, instead of as presently an offset process that takes more time. Some of the information on the original bulletins has been suppressed, though the missing information can be obtained annually in IAGA Bulletin 32. The indices are also published monthly in NOAA's Solar-Geophysical Data. Yearly diagrams of the an, as, am, Dst, and (an - as)/2 curves have been published in IAGA Bulletin 32 since 1976. Similar yearly diagrams for the period 1957-75 have been published in IAGA Supplementary Bulletin 39. Those wishing to use an or as can convert Kn or Ks using the weights p given in Table C2 of "Indices Kn, Ks et Km, 1964-67" by P.N. Mayaud, ed., du C.N.R.S. Paris, 1968.

Note: The new tables give - o + values instead of 3 Km's as in previous tables.

From January 1, 1979, the southern observatories used in the derivation of the as index will be spread into four groups instead of three. This will reduce the small artificial daily variation in the existing as index. A full description of this modification will be published shortly in a book by P.N. Mayaud "Derivation, meaning and use of geomagnetic indices" that will be announced in the IAGA News and IUGG Chronicle. The current technique using three groups will still be used in all the necessary monthly sheets if K indices have not reached Paris when the provisional monthly indices are derived. The change is only of import when detailed statistical studies are required. A brief description of these indices will be found in the URSI Handbook, p. 300, section 13.59. Since the Handbook was issued these indices have largely replaced Kp. The main reason for changing from Kp to Km for a worldwide index is that the original selection of stations used to form Kp was almost entirely confined to the Northern Hemisphere, with the result that Kp has a strong UT variation associated with the concentration of magnetic activity over North America. Km does not suffer from this disadvantage. In general there are significant differences between Kn, Ks, and Km, apparently due to a tendency for major magnetic perturbations to be largely in the winter hemisphere and to small perturbations in summer spreading through the sunlit zone of the ionosphere. When purely local phenomena are the main object of an analysis, local K is often more valuable than the international parameters, particularly for studies of local substorm activity.

VIII. Uncle Roy's Column

The examples given below were all taken from a short length of film showing ionograms made at Maui on January 13, 1979, 0100 LMT to 0700 LMT. They illustrate rather nicely how a number of interesting points can be found even on a short sequence.

(i) Round-the-time base traces

I am occasionally asked whether the order of round-the-time base (RTB) traces can be found quickly. See Fig. 1.9b, p. 15, UAG-23A. In practice this is very simple, and the method is shown below using the Maui ionograms for 0145 and 0315 LMT, Figs. 1 and 2.

For these examples, the equipment is operated with 60 pulses/sec. so that successive ground-wave pulses are separated by 2500 km. If 50 pulses/sec. had been used, the equivalent separation would have been 3000 km.

The value of h'F at 2.0 MHz, where the RTB traces are first seen is about 260 km (the second-order trace is slightly lower than is consistent with the first and high-order traces. This is most probably due to the presence of a TID perturbation). An o trace can be seen at about 80 km, i.e., a total virtual height of 2580 km. Dividing by 260 (h'F at 2.0 MHz) shows that this is a tenth-order trace from 258 km mean height. The next order appears at 300 km, equivalent to 2800 (2500 + 300). Dividing by 260, the nearest factor is 11. $11 \times 260 = 2860$. Clearly this trace is an 11th-order trace at most probable virtual height $2800/11 = 255$ km. Either could have been used to establish the order.

The second example at 0315 shows the same procedure when the RTB traces are steep. This example is also more difficult than usual as the layer is very low, so that the height should be estimated to the nearest 5 km. At 3 MHz, h'F = 210 km and the first clear order is at 100 km, i.e., a range of $2500 + 100 = 2600$ km, $2600/210 = 12.4$, i.e., this is probably a 12th-order trace at an average virtual height of 217 km. We could have used the highest order visible, normally the 14th order if our estimate is

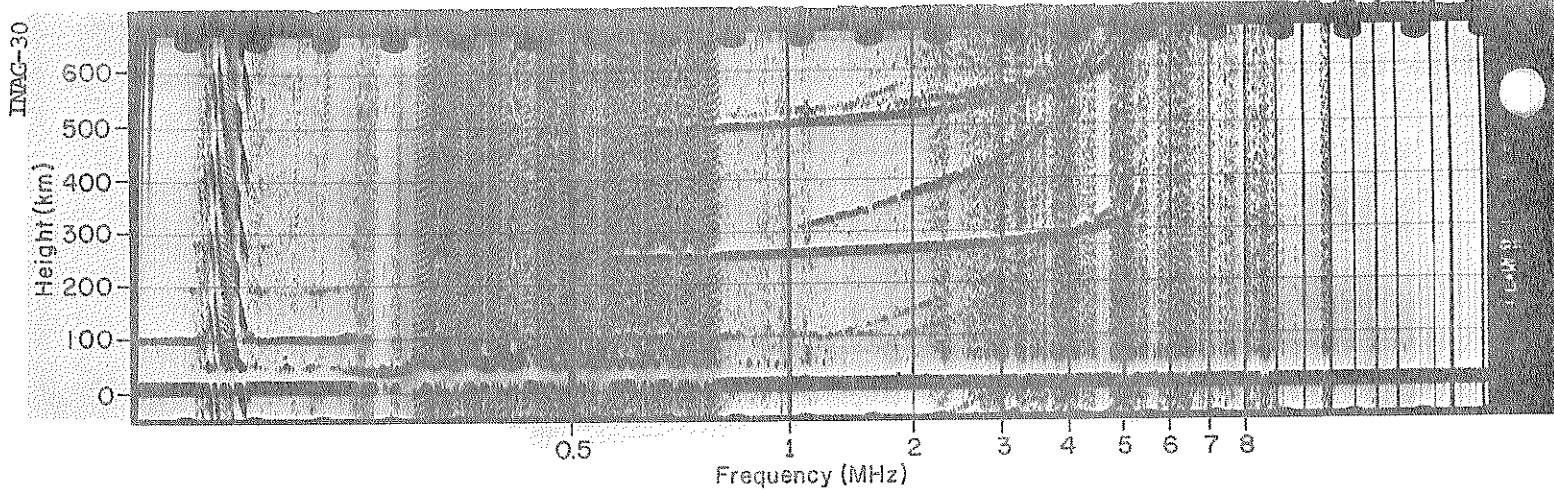


Figure 1. Maui, Jan. 13, 1979, 0145 UT.

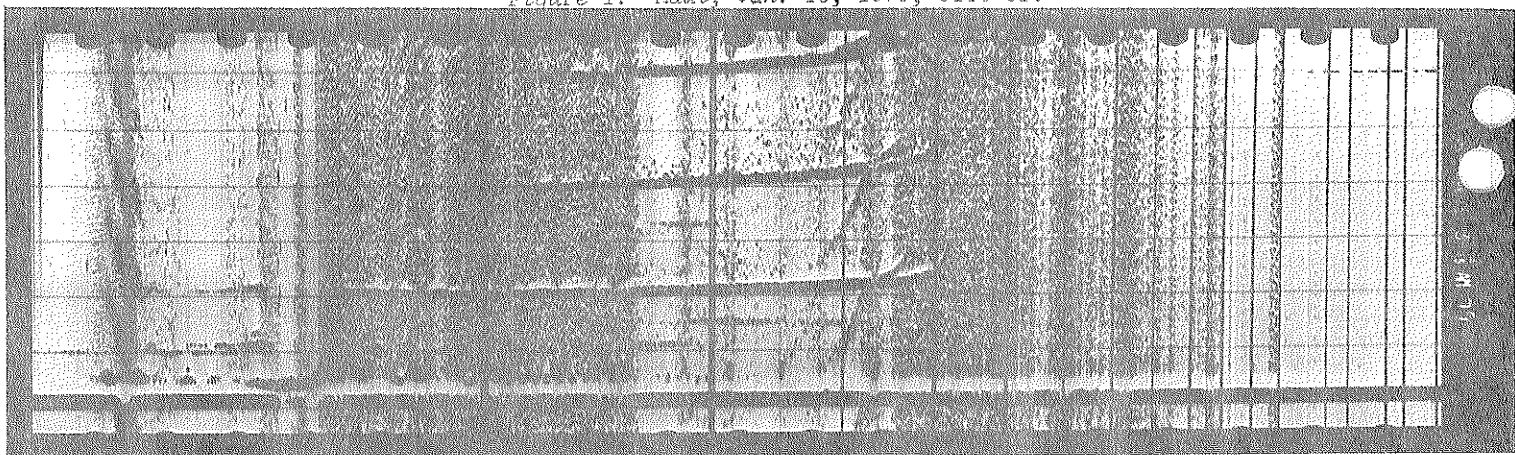


Figure 2. Maui, Jan. 13, 1979, 0315 UT.

right. This is at a height of 520 km, equivalent to $2500 + 520 = 3020$ km, i.e., an average virtual height of 216 km in good agreement with our previous estimate. If the first trace had really been of 13th order, its average virtual height would have been 200 km. The check trace would be 15th order also at 201 km. However, there is no possibility that the virtual height of the low-order traces at 2 MHz (210 km for 1st order, 420 km for second) could be as low as this. Our first estimate is proved to be correct. In my experience it is very unusual for a check of this type to be necessary--usually only one order is possible with much larger safety margins. It is often convenient to pick a frequency at which $h'F$ is a convenient number, 250, 300, or 350 km, for example, so that the order can be mentally calculated.

(ii) foEs Evaluation

The O230 ionogram, Fig. 3, shows two Es traces at different apparent virtual heights. The F trace suggests that $fbEs$ is O80US, RTB traces shows very low absorption so that weak traces should be easily visible. Should $foEs$ be deduced from the upper or lower Es trace? The previous ionogram was very similar except that the upper Es trace and the M reflection trace (2F-Es) were absent. For this $h'Es$ was O95. Noting that the upper Es trace does not blanket the F trace and that the M trace is about 95 km below the 2F trace, it is most likely that both these traces are really a denser Es seen at oblique incidence. As a matter of interest, the pattern corresponds to an Es patch about 8 km from the vertical with a critical frequency at least 2 MHz greater than that overhead. The top frequency of the lower trace must be $fxEs$ and is near 1.8 MHz. The corresponding value of $foEs$ is O13JS with $h'Es = O95$. This is confirmed in the next ionogram (Fig. 4) 15 minutes later in which the upper trace has fallen to about 105 km, the M reflection has become very weak, and an N (F+Es) trace is present about 100 km above the F trace. This is still oblique, as $fbEs$ is still about 0.8 MHz whereas for an Es capable of giving the N reflection, it should be close to $foEs$ (2.5 MHz). The relatively strong o-trace near 1.2 MHz seen on Fig. 3 has vanished as has the second order z trace below 0.5 MHz. The most probable value of $foEs$ overhead is O09US though the edge of the Es sheet with $fxEs = O30$ cannot be more than 2 km from overhead. This illustrates the frequently made point that very little deflection from the vertical can allow $foEs$ to increase significantly. It is a good rule that if $foEs-fbEs$ is large compared with $fbEs$ for a solid trace, the trace is really oblique, but the value of $foEs$ represents the densest part of the Es sheet within a few km of overhead. Many ionogram analyzers find it difficult to understand how a relatively strong trace can exist to $foEs$ and yet $fbEs$ be small. The examples show what is happening fairly clearly.

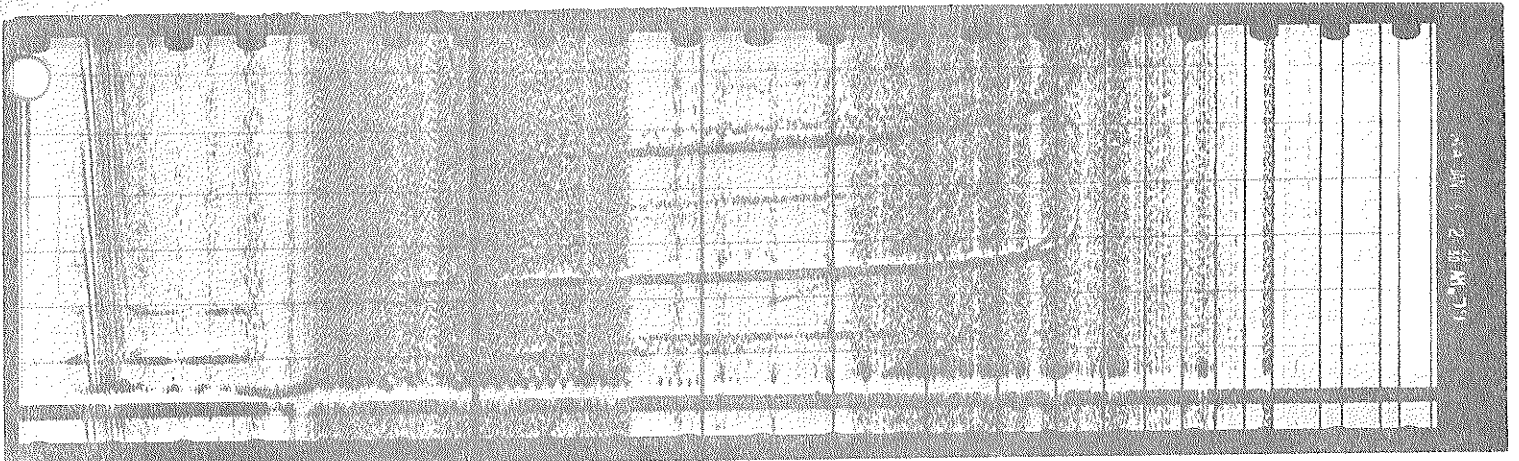


Figure 3. Maui, Jan. 13, 1979, 0230 UT.

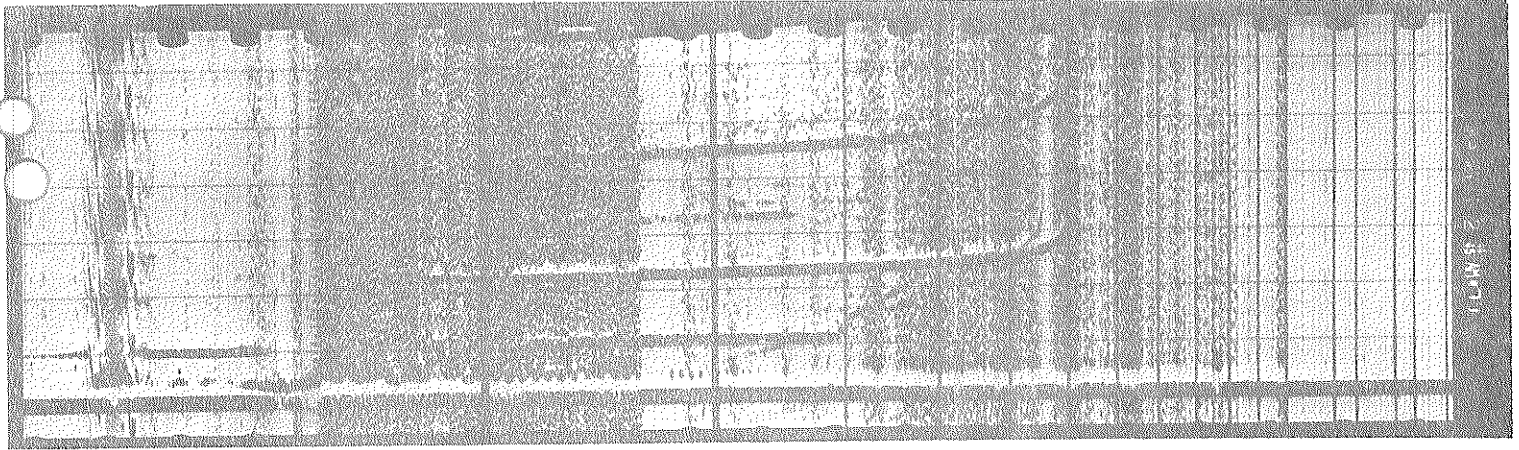


Figure 4. Maui, Jan. 13, 1979, 0245 UT.

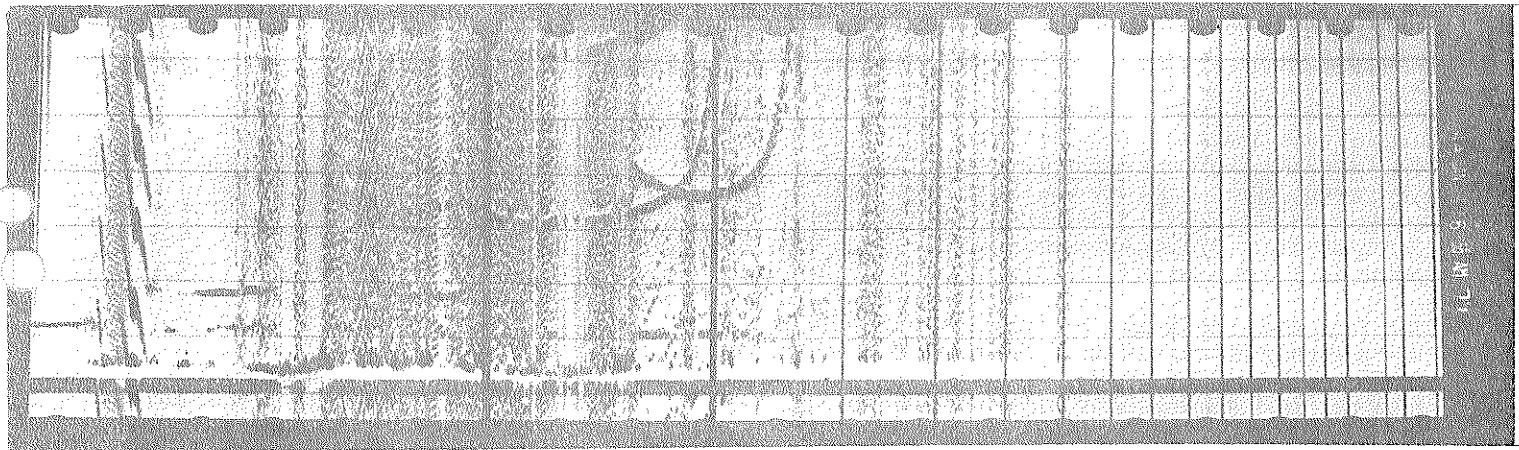


Figure 5. Maui, Jan. 13, 1979, 0600 UT.

(iii) F layer tilt effects near sunrise

When foF2 increases rapidly with time, considerable tilts in the ionosphere can develop and the shape of the F trace is distorted. In these circumstances the sounding is definitely nonvertical and, in general, N(h) computation is not possible without correcting for the effects of the tilt.

Fig. 5 shows the ionogram for 0600 when foF2 was just greater than 2 MHz. An hour later it had reached 5 MHz. The small amount of second-order F trace present shows that the reflection is overhead. The F layer traces at 0700, Fig. 6, are again very nearly overhead, though the exact shape suggests a little residual deviation near foF2. The values of h'F at 0600 and 0700 are above 305 km and 280 km respectively, with probably appreciable retardation in lower ionization present in the former case (h'Fx is sufficiently about fB for gyro retardation to be small so h'Fx-h'F at corresponding frequencies gives a good measure of this). Examining the patterns for 0630, Fig. 7, the o trace is

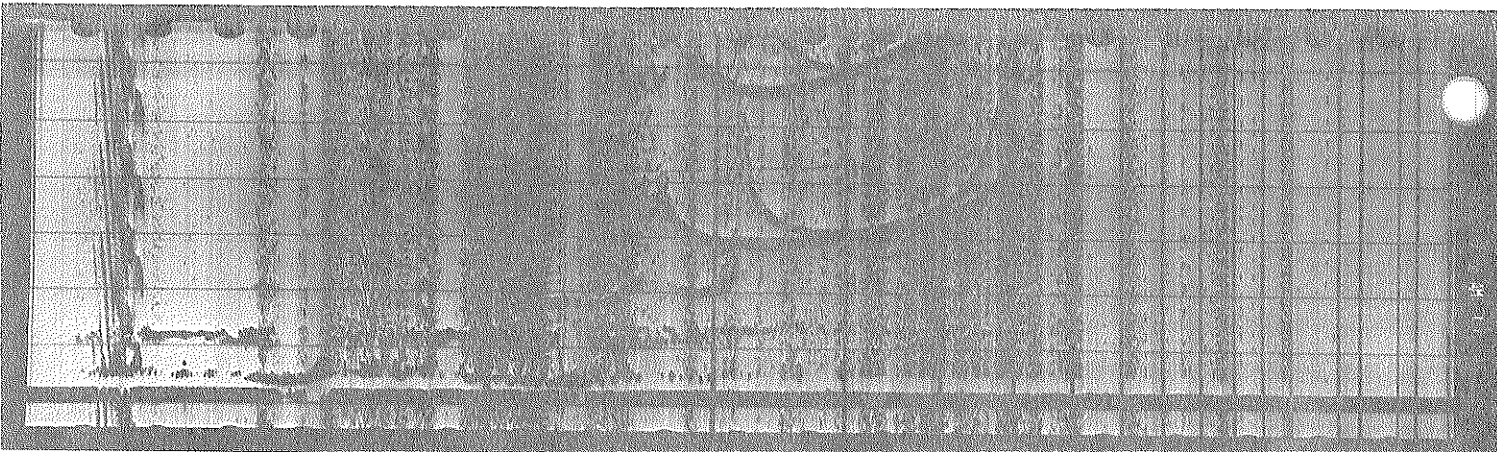


Figure 6. Maui, Jan. 13, 1979, 0700 UT.

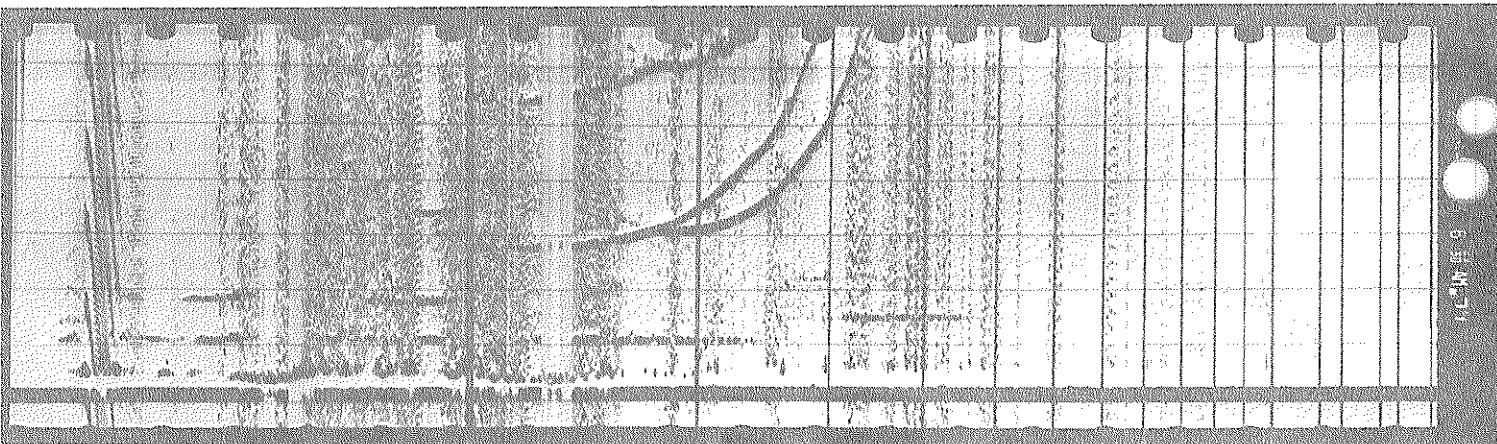


Figure 7. Maui, Jan. 13, 1979, 0630 UT.

overhead up to the point where o and x traces touch, but then starts to go oblique ($2 \times h'F/2F$). However, the shape of the F2 trace is markedly different from the reference patterns. The fact that o and x traces are very similar in shape shows that the tilt is predominantly in the east-west plane (a north-south component for this tilt would make them different). The model is that of Fig. 2.5(a), p. 40, UAG-23A, electron density ranging rapidly with distance. It is likely that a small drop in km also is present (Fig. 2.5 (b)) but this is swamped by the change in N. These three ionograms illustrate the anomaly shown in Fig. 3.34, p. 96, UAG-23A for use of Y. $foF2 = O3OEY$, $M3000 = Y$. $h'F$ is about 280, $1/2 h'2F$ about 270 km, showing that the tilt near the bottom of the layer is small (the reflection point is about 5 km off vertical whereas it is between 10 and 20 km or more for the distorted trace.)

The fact that the height $h'F$ is a slant height is shown conventionally by $-H$, UH , or EH as allowed by the accuracy rules, $-Y$ etc., is acceptable but is really intended for severe tilt as shown in the higher parts of the traces. In this case, with a height accuracy of ± 5 km, UH is appropriate. Judging from the true sequence the turnover given for $foF2$ in Fig. 3.4 of UAG-23A would occur at heights of about 1000 km with $foF2$ limit value near 3.7 MHz!

Rather similar ionograms are found under the steep slopes of the equatorial anomaly ridges. However, the low dip decreases the effects of north-south gradients on the relative shape of o and x traces so it is not easy to distinguish between north-south and east-west tilts. In this case the spatial gradients are relatively slowly varying with time and distorted traces may be present for many hours with relatively little change in shape with time. Much care is therefore needed when deducing $M3000$ or profiles from such ionograms. The height of the maximum of the layer looks much higher than it really is.

IX. Training Aids

INAG has, in the past, published a number of excerpts from training aids; see, for example, correspondence course, but these have mainly come from one or two groups. There are at least 10 groups operating three or more stations, most of whom must have training problems. Why not share them with the community?

X. Correspondence Course

Problems in the Identification of foE

This note on the identification of foE was originally drawn up by Richard Smith of WDC-C1, but has been developed for use in the annual training course of the British Antarctic Survey.

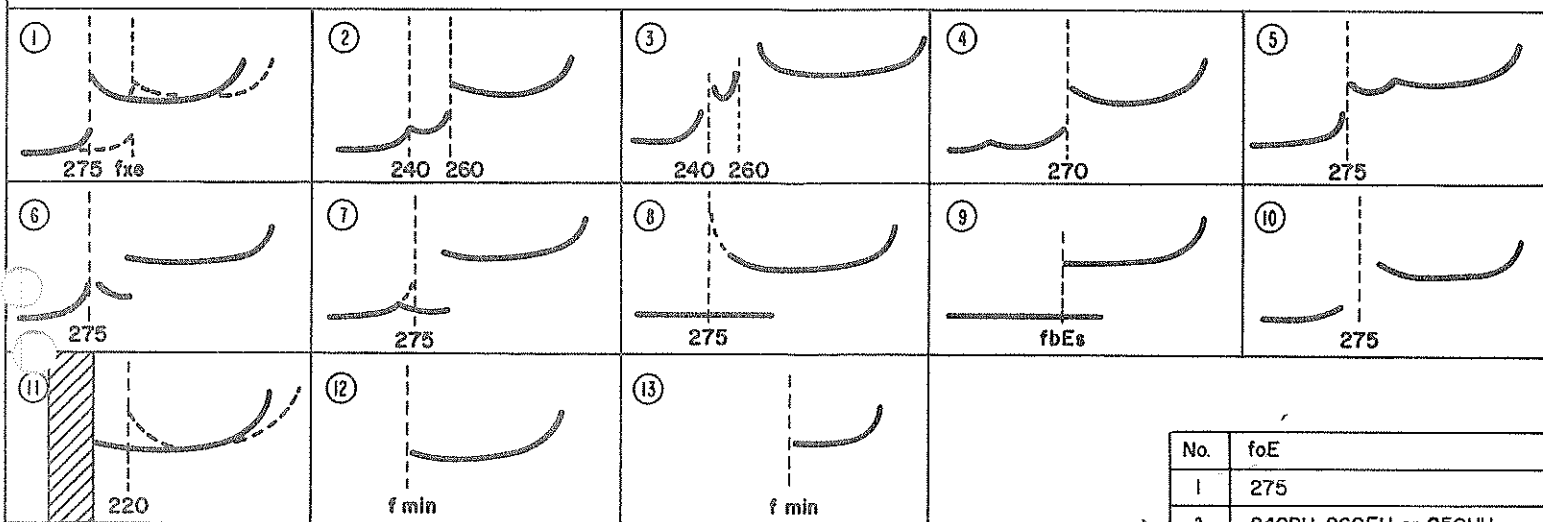
Problems in the identification of foE can occur when there is blanketing by an Es layer, or in conditions when the measurement has been influenced by absorption. But perhaps the greatest difficulty arises when additional critical frequencies are present in the vicinity of foE. These can arise from either the effects of a traveling ionospheric disturbance (see UAG-23A, p. 47) or the presence of an E2 layer. The latter often appears about sunrise and can last all day at some observatories.

The way to resolve the problem is to examine the sequence of ionograms on either side, or, if this fails, use data from surrounding days to determine the approximate value of foE for that local time. It should be remembered that foE which is very strongly solar-controlled, varies smoothly through the day with a maximum about local noon. Another identification of the expected value of foE can be obtained from the value of foF1. The ratio of foF1 to foE varies from about 1.3 to 1.7 over the world but at any location the ratio is remarkably constant for much of the time when both layers are observed.

At low and middle latitudes the value of foE is hardly affected even during intense magnetic storms. At high latitude, significant enhancements in ionization can occur as a result of particle precipitation. This enhanced layer is called particle E and the scaling rules for these occasions can be found in UAG-23 or 23A, Chapter 4.

A very real problem arises at some stations where the E pattern near sunrise shows a ladder structure with no dominant cusp. Very good examples have been given in the High Latitude Supplement, p. 59, Fig. 2.23. Physically the most significant cusp-let is the highest one which forms part of E trace rather than a stratification of the F trace. In this type of situation, there is no real valley between E and F and the definition of foE is physically not very meaningful.

Fig. 8 below shows the British Antarctic Survey Training Aid.



No.	foE
1	275
2	240DH, 260EH or 250UH
3	240-H
4	270-H
5	275
6	275
7	275UA, 275DA
8	275UA
9	(fbE ₃) EA, A
10	275UR
11	160JS for fB = 1.2 MHz
12	fmin EB
13	B

Identification of foE

Figure 8. British Antarctic Survey training aid for ionogram analysis.

1. $f_oE = 275$. Note that the extraordinary component is usually weaker than the ordinary, and at times of increased absorption (high f_{min}) the x component may not be visible. The x component of the normal E trace should not be confused with Es when the turn up at f_xE is missing.
2. Use $f_oE = 240DH$, $260EH$, or $250UH$, whichever fits in with a smooth diurnal variation. See remarks in the opening paragraphs.
3. This illustrates the presence of an E2 ionogram. f_oE is always taken as the lower critical frequency ($f_oE = 240-H$), in these circumstances.
4. The low frequency stratification is clearly not f_oE which should be scaled $270-H$. The descriptive letter H shows that a stratification is present but is not affecting the evaluation of f_oE .
5. $f_oE = 275$. The stratification is in the F region and f_oE is the lower cusp value. The presence of the stratification should be indicated on h'F.
6. This is an example of high type Es (Es-h). As this occurs above the maximum height of E, the cusp frequency is equal to f_oE .
7. This is an example of cusp type Es (Es-c) which occurs within the normal E layer, i.e., below the maximum electron concentration. Therefore the frequency of the cusp is less than f_oE . In many cases the trace can be extrapolated to f_oE but should be qualified, depending upon the difference between the cusp frequency and the extrapolated value of f_oE . In this case either 275UA or 275DA would be acceptable.
8. The normal E trace has been blanketed by low type Es but there is curvature at the bottom of the F trace. Use extrapolation if the curvature is sufficient.
9. Again use the qualifying letters as in 7. Either (fbEs)EA or A would be the most likely scalings for f_oE .
10. High absorption around the critical frequency (R) prevents f_oE from being seen. If this absorption band is less than 4% of the critical frequency or $\pm\Delta$, whichever is the greater, the center frequency may be scaled and described by R; if between 4 and 10% or $\pm 2\Delta$ the qualifying letter U should be used. However, if the band is 10 to 20% of the center frequency use the highest frequency of the normal E trace followed by DR. If the band is more than 20% (unusual) use R.
11. This pattern often occurs around sunrise and sunset. The ordinary E trace and the retardation at the bottom end of the ordinary F trace are obscured by interference. However, the retardation of the F ordinary component can be seen just above f_xE . Use $(f_xE - f_B/2)JS$ for f_oE . (f_B is the gyrofrequency). Note: Sometimes when D region absorption is low (around sunrise, sunset), the extraordinary F trace shows retardation (curvature) due to the gyrofrequency f_B . This can be mistaken for an E-layer critical frequency. A good check is to look at succeeding records where the gyrofrequency retardation will stay constant in frequency, whereas f_xE decreased rapidly near sunset and increased near sunrise.
12. This is an example of high D region absorption (B) giving an f_{min} near enough to f_oE to also affect the F trace. Use $(f_{min})EB$ for f_oE .
13. Here there is no sign of retardation at f_{min} . Use $f_oE = B$ provided the normal E region would usually have been present at this hour.

Note that in examples 1, 11, and 12 it is very important to resolve whether the retardation at the low frequency end of the F trace indicates the normal E layer, a particle E layer, a stratification, or the presence of an E2 layer.

XI. Electron density-height problems

For many years there has been much controversy on how best to obtain the variation of electron density with height from an ionogram and a large number of methods have been developed for this purpose. In general, there are three major factors to be considered:

- (a) The inversion problem is very complicated and difficult so, with perfect ionograms, accuracy depends primarily on the degree of complexity that may be accepted.
- (b) Methods that are tailored to match the type of $N(h)$ profile actually present in a given theater should, in general, give greater accuracy for a given effect than those that are not, but at the expense of greater errors when this condition is not present.
- (c) In practice, there are experimental errors in actual ionograms, absorption, and screening (e.g., from Es) that prevent some of the data needed for an accurate solution from being observed and tilts in the ionosphere invalidate the basic assumption that the sounding is vertical.

This wide range of conditions that can occur at any station offers at least an a priori argument in favor of testing all methods against a very wide range of models and this has been done in the international analysis reported below. Where adequate computers are available there is much to be said for selecting one of the "best" methods. Where ionogram quality, absorption, or screening are important for the majority of the ionograms to be inverted, the best available accuracy can be surprisingly good and economy would then indicate that a simpler method could be adequate. This is the reason why simple methods have been surprisingly effective--particularly for the determination of hmF2. It should be noted that certain limitations are common to all methods, e.g., the curvature of the profile near the maximum of a layer, and thus the apparent thickness of the layer peak, is very sensitive to small errors in determining the critical frequency, e.g., a 1% error in foF2 can alter the apparent thickness by a factor of about 30%.

On behalf of the users, INAG would like to thank Dr. McNamara for his great efforts and skill in getting a consensus from a group of workers who are rather notorious for bitter controversy. INAG is very pleased to publish this summary of the full report UAG-68 "A Comparative Study of Methods of Electron Density Profile Analysis," prepared by Dr. McNamara on this page.

As chairman of INAG, I would like to draw your attention to the new Handbook of N(h) profile analyses based on POLAN which is being prepared by Dr. McNamara. As with our publications, this should be illustrated with actual ionograms from many parts of the world so as to show both ionogram and equivalent electron density profile.

For this purpose, Dr. McNamara needs good quality typical ionograms. INAG has already requested similar ionograms to illustrate the Handbook--as requested by many INAG users. So far none have been submitted. It is impossible for either Dr. McNamara or your chairman to meet your needs unless you collaborate by providing them with suitable ionograms. Please act now. It is obviously more valuable if we have both the profile and the ionogram for future discussions so Dr. McNamara and myself will collaborate whenever possible.

Typical ionograms suitable for N(h) analysis in particular with

- (a) minimum Es screening
- (b) good height and frequency accuracy
- (c) well-defined retardation patterns should be sent to:

Dr. Leo McNamara
Ionospheric Prediction Service
162-166 Goulburn Street
P.O. Box 702
Darlinghurst, N.S.W. 2010, Australia

For those of you with no activity in N(h) work, this is an exceptional opportunity to find out what your ionosphere really looks like! Act!!

Summary of a Comparative Study of Methods of Electron Density Profile Analysis

by

L.F. McNamara, Chairman, URSI WG G/5

Subgroup G/6/2 of Working Group 6, Commission G of the International Union of Radio Science (URSI), was formed after the 17th URSI General Assembly in Warsaw, 1972. Subgroup G/6/2 was asked to compare extant methods of real-height analysis of ionograms in order to recommend the "best" technique(s).

Experts in the field who composed the subgroup attempted to compare all known available methods. The comparisons were made on the basis of the accuracy of the results obtained by each method in the analyses of a series of accurate numerical ionograms, with the correct results being known only to the chairman. Of those methods for which sufficient results were presented to allow definitive conclusions to be drawn, those of A.K. Paul (Boulder, CO, USA) and J.E. Titheridge (Auckland, N.Z.) proved to be the most promising.

The test ionograms considered separately the problems caused by lack of echoes below fmin (the starting problem) and by the presence of a valley between the E and F layers. A summary of the results has been published in the WDC-A for STP Report UAG-68. This report also shows how the field has developed over the past 10 or so years since the Radio Science Special Issue on Analysis of Ionograms for Electron Density Profiles was published in October 1967.

The different methods of analysis considered are discussed in UAG-68 mainly in terms of their

accuracy as indicated by their results for the test ionograms. Other important aspects of the problem, as far as the use of the methods by persons other than the originators is concerned, are the availability of the computer program, the ease with which the program may be applied routinely, and the computation time for each complete analysis. These topics were discussed at a meeting of the subgroup in Helsinki, preceding the 19th URSI General Assembly.

Methods of analysis discussed in UAG-68 are those used by L. Bossy, W. Becker, J.E. Titheridge, A.K. Paul, T.L. Gulyaeva, and H.H. Howe and D.E. McKinnis, as used by J.W. Wright. Although a set of tests conducted before 1975 also included results for the methods of O.A. Mal'tseva, A.K. Saha, and J.E. Jackson as used by J.E. Bennett and J.S. Nisbet, these three techniques are not reconsidered because the Mal'tseva and Jackson methods were found to be significantly less accurate for the pre-1975 tests than the former set of methods, and Saha did not provide results for the second set of tests.

For those members of the subgroup who completed all or most of the tests, the effort has been a learning process, the methods and computer programs being continually modified to perform better in following tests. In fact, neither of the most successful programs, Titheridge's POLAN nor Paul's complicated method program, has yet reached its final stage. It is thus not possible to recommend a "best" method of N(h) analysis, although it is obvious that these two methods are the most promising.

Only Paul and Titheridge obtained good results for the valley tests, so the Gulyaeva and Howe-McKinnis programs cannot be recommended for general use. However, the latter programs gave good results for the starting tests, and in some cases were more accurate than the Paul or Titheridge (POLAN) method. In fact, there were times when the Paul or Titheridge results were the worst, so both of these methods have their limitations.

If Paul's or Titheridge's method is used to analyze accurate nighttime ionograms with suitable x traces, the height of the base of the F layer can generally be determined to within about 5-10 km. If either of these techniques is used to analyze an accurate daytime ionogram with suitable x traces, the height of the F-layer base can be determined to within a few kilometers. Larger errors must be expected in the analysis of real ionograms, which introduce experimental errors. In fact, methods of N(h) analysis seem to have reached the stage where the accuracy of the results is limited by the quality of the input data, at least for analysis of conventional film ionograms.

At the time of writing, Titheridge's POLAN is more readily available and better documented than Paul's program. They require about the same computer storage and have very similar computation times. For some users, POLAN's "one-pass" solution may be an important consideration--at present Paul's program still requires visual inspection of the results to determine whether further iteration is necessary.

Computer programs and documentation will be available both from the originators and WDC-A for STP in the near future. Some descriptions of POLAN are given by Titheridge in Appendix A of UAG-68.

For organizations with only small computer facilities, POLAN or Paul's complicated method (as used in the present tests) may be too large, in which case recourse must be made to programs such as Titheridge's simpler program LAPOL or Paul's earlier "simplified method for use with minicomputers." For these particular programs, accuracy of the results has been traded off in favor of simplicity, the starting and valley corrections being rather unsophisticated.

Because of their limited accuracy, Titheridge's single polynomial method and the Schmerling 10-point method should be used only when suitable computer facilities are not available. If possible, attempts should be made to implement at least Titheridge's program, LAPOL, or Paul's simplified method, both of which introduce simple underlying ionization and valley corrections and are smaller and faster than the more sophisticated methods.

Subgroup G/6/2 was renamed at Helsinki as Working Group G/5 "Evaluation of Analysis Techniques in Ionospheric Research."

XII. Index to Contents of NOAA's Monthly Solar-Geophysical Data by Discipline

The following table gives the disciplines and subdisciplines in accordance with the "Guide to International Data Exchange through the World Data Centers," prepared by the ICSU Panel of World Data Centres. The fourth consolidated version is in press.

DETAILED DATA COVERAGE FOR SOLAR GEOPHYSICAL DATA

<u>A. Solar and Interplanetary Phenomena</u>		<u>Mo/Yr</u>	<u>Mo/Yr</u>
A.1	Sunspot Drawings	1/67	- present
A.1a	Sunspot Data (see A.5a)	7/57	- present
A.2a	Zurich Provisional Relative Sunspot numbers, Rz	7/57	- present

A.2b	Zurich Final Sunspot numbers, Rz	7/57 - present
A.2c	American Relative Sunspot numbers, RA'	7/57 - present
A.2d	27-day Plot of Relative Sunspot numbers (see D.1c)	7/57 - present
A.2e	Sunspot Cycle (Smoothed Numbers) Graphs -- in each issue	7/57 - present
A.2f	Table of Observed and Predicted Smoothed Sunspot numbers	10/64 - present
A.3a	Mt. Wilson Magnetograms	9/66 - present
A.3b	Mt. Wilson Sunspot Magnetic Field Classifications	1/62 - present
A.3c	Kitt Peak Magnetograms	7/74 - present
A.3d	Mean Solar Magnetic Field (Stanford)	1/77 - present
A.3e	Stanford Magnetograms	1/79 - present
A.4	H α Filtergrams	1/67 - present
A.5	Calcium Plage Drawings - McMath (or Catania)	1/67 - present
A.5a	Calcium Plage (McMath) and Sunspot Regions	7/57 - present
A.5b	Daily Calcium Plage Index	12/70 - present
A.6	H α Synoptic Charts	6/73 - present
A.6b	Synoptic Chart and Active Regions	4/76 - present
A.6c	Stanford Solar Magnetic Field Synoptic Charts	1/79 - present
A.7a	Coronal Line Emission Indices (Provisional)	7/57 - 5/66
A.7b	Coronal Line Emission Indices (Final)	1/60 - present
A.7c	White Light Corona (NRL OSO-7, 1971-083A)	2/72 - 6/74
A.7e	Solar XUV Coronagrams (NRL OSO-7, 1971-083A)	10/72 - 12/73
A.7f	Helium D3 Coronal Holes (Big Bear)	1/76 - present
A.7h	λ 5303Å Coronal Intensities (Sac Peak or Wendelstein)	1/77 - present
A.8aa	2800 MHz (ARO-Ottawa) Daily Observed Values of Solar Flux	7/57 - present
A.8ab	2800 MHz (Ottawa) Final - Daily Observed Values of Solar Flux	1/62 - 12/66
A.8ac	2800 MHz (ARO-Ottawa) Daily Values Solar Flux Adjusted to 1 A.U.	1/64 - present
A.8ad	2800 MHz (Ottawa) Final - Daily Values of Solar Flux Adjusted to A.U.	1/64 - 12/66
A.8b	470 MHz (Boulder) Daily 3-hourly Averages	7/57 - 3/58
A.8c	167 MHz (Boulder) Daily 3-hourly Averages	7/57 - 12/58
A.8d	200 MHz (Cornell) Daily 3-hourly Averages	7/57 - 12/58
A.8e	9530 MHz (USNRL) Daily Averages	2/58 - 4/59
A.8f	3200 MHz (USNRL) Daily Averages	2/58 - 4/59
A.8g	15400, 8800, 4995, 2695, 1415, 606, 410, 245 MHz (AFGL) Solar Flux Adjusted to 1 A.U. (15400 MHz began 6/69, 245 MHz began 10/69, 410 MHz began 9/71)	1/67 - present
A.9a	9.1 cm (Stanford) Radio Maps of the Sun	4/60 - 8/73
A.9aa	9.1 cm Spectroheliogram tabulated Data (Stanford)	1/69 - 8/73
A.9b	21 cm (Fleurs) Radio Maps of the Sun	12/64 - 12/73
A.9c	8.6 mm (Prospect Hill) Radio Maps of the Sun	4/70 - 2/74
A.9cb	8.6 mm (NOSC) Radio Maps of the Sun	11/74 - 9/78
A.9d	2 cm (NOSC) Radio Maps of the Sun	6/74 - 9/78
A.10a	169 MHz (Nancay) Interferometric Observations	7/57 - present
A.10b	408 MHz (Nancay) Interferometric Observations	11/65 - 8/71
A.10c	21 cm (Fleurs) East-West Solar Scans	10/65 - present
A.10d	43 cm (Fleurs) East-West Solar Scans	4/66 - present
A.10e	10.7 cm (Ottawa-ARO) East-West Solar Scans	6/68 - present
A.10f	3 cm (Toyokawa) East-West Solar Scans	1/78 - present
A.11aa	Solar X-ray Background Levels (NRL) satellites, see below	1/64 - present
A.11ab	Solar X-ray Background Levels (NRL Graphs) " " "	3/65 - present
A.11ac	Solar X-ray Background Levels (Boulder) " " "	12/65 - 11/68
A.11ad	Solar X-ray Background Levels (France) " " "	4/66 - 5/66
A.11ae	Solar X-ray Background Levels (Aberdeen, S.D.) " " "	1/66 - 11/68

Popular Name	Satellite Designation	
SOLRAD 7A	1964-1D	1/64 - 10/64
SOLRAD 7B	1965-16D	3/65 - 12/65
SOLRAD 8	1965-93A	
(Explorer 30)		1/66 - 12/67
OGO-4	1967-73A	1/68 - 3/68
OSO-4	1967-100A	
SOLRAD 9	1968-17A	3/68 - 7/72
(Explorer 37)		6/73 - 4/74
(Beginning 12/68 daily/hourly averages presented)		
SOLRAD-10	1971-58A	8/72 - 6/73
(Explorer 44)		
SOLRAD-11	1976-023D	1/78 - present

A.11b	Solar X-ray Background Levels, 0-20Å Injun 1/SOLRAD-3, 1962-02	6/61 - 12/61
A.11c	Solar X-ray Background Levels (Vela 1,2; 1963-39A,C)	(10/63)

A.11d	Solar X-ray Background Levels (McMath (OSO-3; 1967-20A), 8-12A)	3/67 - 8/67
A.11e	Solar X-ray (OSO-5; 1969-6A) Spectroheliograms (University College London, Leicester Univ.)	7/69 - 11/72 7/74 - 6/75
A.11f	Solar X-ray (GSFC OSO-7, 1971-083A) Spectroheliograms	12/72 - 7/74
A.11g	Solar X-ray Background Levels (SMS-1/GOES, 1974-033A; SMS- 2/GOES, 1975-011A)	1/74 - 12/78
A.11h	Solar X-ray (OSO-8, 1975-057 A) 2-14 keV (Lockheed)	8/75 - 9/78
A.11i	Solar X-ray (OSO-8, 1975-057A) (Columbia University)	
A.11ja	Solar EUV Spectroheliograms FeXV Å (GSFC OSO-7, 1971-083A)	5/72 - 3/74
A.11jb	FeXV - 284Å Spectroheliograms	2/76 - 12/76
A.12aa	Solar Protons, Daily-hourly Values, JPL/GSFC (satellites, see below)	5/67 - 5/73
A.12ab	Solar Protons, Graphs, JPL/GSFC " " "	5/67 - 5/73
	Popular Name	Satellite Designation
	Explorer 34	1967-51A, EP >10, >30, >60 Mev
	Explorer 41	1969-53A, EP >10, >30, >60 Mev
	Explorer 43	1971-19A, Ep >10, >30, >60 Mev
		5/67 - 5/69 6/69 - 12/72 11/71 - 5/73
A.12ba	Cosmic Ray Protons, Ep 0.6-13, 13-175, >175 Mev, Univ. of Chicago (Pioneer 6; 1965-105A and Pioneer 7; 1966-75A)	3/69 - present
A.12bb	Cosmic Ray Protons, Ep >13.9, >64 or >40 Mev, Univ. of New Hampshire (Pioneer 8; 1967-123A and Pioneer 9; 1968-100A)	12/69 - present
A.12c	Cosmic Ray Protons, Ep 5-21, 21-70 Mev, Aerospace (ATS-1; 1966-110A)	1/70 - 8/72
A.12d	Low Energy Protons (NOAA satellites 1972-082A, 1973-086A, 1974-089A)	7/74 - 11/74
A.12e	Energetic Solar Particles (IMP H, 1972-073A and IMP J, 1973-078A)	8/75 - present
A.12f	Energetic Solar Particles (GMS/SEM, 1977-065A)	9/77 - present
A.13a	Solar Wind (Pioneer 6, 1965-105A; and Pioneer 7, 1966-75A) NASA Ames	12/65 - present
A.13ab	Solar Wind (Pioneer 8, 1967-123A; Pioneer 9, 1968-100A) NASA Ames	4/72 - present
A.13b	Solar Wind, M.I.T. Pioneer 6, 1965-105A	3/69 - 2/70 12/73 - present
	Pioneer 7, 1966-75A	6/69 - 12/69
A.13c	Solar Wind (Vela 3, 1964-40A; Vela 5, 1965-58A)	1/69 - 6/72
A.13d	Solar Wind from IPS Measurements (UCSD)	1/75 - present
A.13e	Solar Plasma Data (IMP H, 1972-073A and IMP J, 1973-078A)	8/75 - present
A.17	Interplanetary Magnetic Field Pioneer 8, 1967-123A	10/72 - present
	Pioneer 9, 1968-100A	4/72 - present
A.17c	Inferred Interplanetary Magnetic Field	12/71 - present
A.18	Interplanetary Electric Field Pioneer 8, 1967-123A	5/72 - present
	Pioneer 9, 1968-100A	4/72 - present
B. <u>Ionospheric (and Radio Wave Propagation) Phenomena</u>		
B.10	Radar Meteor Indices, perpetual, based upon 1958-1962 data for N45 latitude -- see issues 246, 251	
B.51aa	NARWS Quality Figures and Forecasts (NBS/ESSA)	7/57 - 12/65
B.51ab	NARWS Comparison Graphs (NBS/ESSA)	7/57 - 12/65
B.51ba	NPRWS Quality Figures and Forecasts (NBS)	7/57 - 12/65
B.51bb	NPRWS Comparison Graphs (NBS)	7/57 - 10/64
B.51ca	High Latitude Quality Figures and Forecasts (ESSA/OT)	11/64 - 9/76
B.51cb	High Latitude Comparison Graphs (ESSA/OT)	11/64 - 11/73
B.52	North Atlantic Graphs of Useful Frequency Ranges (German PTT)	7/57 - present
B.53	Quality Figures Based Upon Frequency Ranges (German PTT)	1/70 - present
C. <u>Flare-Associated Events</u>		
C.1a	H- α Solar Flares (Preliminary)	7/57 - present
C.1ba	H- α Solar Flares (including Standardization Data) (Divided into Confirmed and Unconfirmed Flares from 1/68-12/74)	9/66 - present
C.1c	H- α Subflares (included in C.1a and C.1b after 1/62)	7/57 - present
C.1d	H- α Flare Patrol (The most recent issue listed for a month contains the comprehensive flare patrol.)	7/57 - present
C.1e	H- α Flare Index (Daily)	9/69 - present
C.1f	H- α Flare Index (by Region)	9/70 - present
C.1g	Frequency of Occurrence of Confirmed Solar Flares	1/68 - 6/68
C.3a	2800 MHz (Ottawa) Outstanding Occurrences	7/57 - present

C.3aa	2800 MHz (Ottawa) Hours of Observation	7/57 - 12/65
C.3b	470 MHz (Boulder) Outstanding Occurrences	7/57 - 3/58
C.3c	167 MHz (Boulder) Outstanding Occurrences	7/57 - 10/60
C.3ca	167 MHz (Boulder) Hours of Observation	1/59 - 12/59
C.3d	200 MHz (Cornell) Outstanding Occurrences	7/57 - 12/58
C.3e	9530 MHz (USNRL) Outstanding Occurrences	2/58 - 4/59
C.3f	3200 MHz (USNRL) Outstanding Occurrences	2/58 - 4/59
C.3g	200 MHz (Hawaii) Outstanding Occurrences	6/59 - 8/59
C.3h	108 MHz (Boulder) Outstanding Occurrences	1/60 - 6/66
C.3ha	108 MHz (Boulder) Hours of Observation	1/60 - 12/65
C.3i	221 MHz (Boeing-Seattle) Outstanding Occurrences (Interferometric) - Changed to 223 MHz in May 1963	4/62 - 7/63 5/65 - 11/65 6/65 - 3/66
C.3j	107 MHz (Haleakala) Outstanding Occurrences	
C.3k	10700, 2700, 960 MHz (Pennsylvania State Univ.) Outstanding Occurrences	7/64 - 5/75 7/66 - 4/69
C.3l	486 MHz (Washington State Univ.) Outstanding Occurrences	
C.3m	18 MHz Bursts (Boulder) (reported with C.6 1/63 - 11/66, C.6ab prior to 1/63)	11/67 - present
C.3n	35000, 15400, 8800, 4995, 2695, 1415, 606, 410, 245 MHz (AFCRL - Sagamore Hill) Outstanding Occurrences (15400 MHz began 11/67, 35000 and 245 MHz began early 1969, 410 MHz began 1971)	1/66 - present
C.3p	184 MHz (Boulder) Outstanding Occurrences	3/67 - 7/72
C.3q	7000MHz (Sao Paulo) Outstanding Occurrences	11/67 - present
C.3r	408 MHz (San Miguel) Outstanding Occurrences	10/67 - 4/72
C.3s	18 MHz (McMath-Hulbert) Bursts	1/68 - present
C.3t	43.25, 80 and 160 MHz (Culgoora) Selected Bursts	12/72 - present

Note: Beginning with the data for April 1966, in CRPL-FB-261, the C.3 entries on Solar Radio Outstanding Occurrences for the Western Hemisphere observatories and frequencies were combined into a single table "Solar Radio Emission Outstanding Occurrences, C.3." Beginning with June 1969 data, the table was expanded to worldwide coverage, and the various observatories are no longer indexed separately.

C.4aa	Solar Radio Spectrograms of Events (Fort Davis)	
	100 - 580 MHz	7/57 - 12/58
	25 - 580 MHz	1/59 - 12/62
	50 - 320 MHz	1/63 - 3/65
	25 - 320 MHz	4/65 - 12/66
	10 - 580 MHz	1/67 - 2/70
	10 - 1000 MHz	3/70 - 4/70
	10 - 2000 MHz	5/70 - 5/73
	10 - 4000 MHz	5/73 - 3/74
	25 - 320 MHz	4/74 - 12/77
	25 - 580 MHz	1/78 - present
C.4ab	2100-3900 MHz Solar Radio Spectrograms of Events (Fort Davis)	1/60 - 12/61
C.4b	Solar Radio Spectrograms of Events (Boulder)	
	7.6 - 41 MHz	3/61 - 8/68
	7.6 - 80 MHz	9/68 - 6/76
C.4c	450-1000 MHz Solar Radio Spectrograms of Events (Owens Valley)	11/60 - 10/61
C.4d	Solar Radio Spectrograms of Events (Culgoora)	
	10 - 210 MHz	1/67 - 7/69
	8 - 2000 MHz	8/69 - 2/70
	8 - 4000 MHz	3/70 - 10/70
	8 - 8000 MHz	11/70 - present
C.4e	30-1000 MHz Solar Radio Spectrograms of Events (Weissenau, GFR)	3/68 - present
C.4f	Solar Radio Spectrograms of Events (AFCRL - Sagamore Hill)	
	19 - 41 MHz	1/68 - 7/70
	24 - 48 MHz	7/70 - 7/75
	25 - 75 MHz	8/75 - present
C.4g	20-60 MHz Solar Radio Spectrograms of Events (Clark Lake)	4/70 - 9/70
C.4h	160-320 MHz Solar Radio Spectrograms of Events (Dwingeloo)	1/74 - present
C.4i	100-1000 MHz Solar Radio Spectrograms of Events (Dürnten)	1/74 - present
C.4j	24-48 MHz Solar Radio Spectrogram of Events (Manila)	4/74 - present
C.5a	Solar X-ray Events (Vela 1,2; 1963-39A,C)	(10/63)
C.5b	Solar X-ray Events (Univ. of Iowa)	
	Explorer 33; 1966-58A (2-12A)	7/66 - 10/71
	Explorer 35; 1967-70A (2-12A)	12/67 - 7/72

INAG-30

C.5c	Solar X-ray Events (NRL Tabulation) (See A.11ab for NRL Graphs and list of Satellites)	1/64 - 10/64 3/65 - present
C.5d	Solar X-ray Events (McMath-Hulbert) OSO-3; 1967-20A (8-12Å)	3/67 - 8/67
C.5e	Solar X-ray Events (SMS-1/GOES, 1974-033A; SMS-2/GOES, 1975-011A)	11/74 - 12/78
C.5f	Solar X-ray Events (OSO-8, 1975-057A) (Columbia University)	
C.6	Sudden Ionospheric Disturbances (SID)	1/63 - present
C.6aa	Sudden Ionospheric Disturbances (SWF) (included with C.6 after 12/62)	7/57 - present
C.6ab	Sudden Ionospheric Disturbances (SCNA, SEA bursts)	1/58 - present
C.6ac	Sudden Ionospheric Disturbances (SPA)	6/61 - present
C.7	Solar Proton Events - Direct Measurement - same as A.12	5/67 - present
C.8	Solar Proton Events - Riometer Confirmed Polar Cap Absorption Events (ESSA)	1/67 - 6/67
C.8ba	Solar Protons, 26 MHz Riometer Events (South Pole) Provisional	9/63 - 11/67
C.8bc	Solar Protons, 30 MHz Riometer Events (Frobisher Bay)	1/65 - 5/65
C.8be	Solar Protons, 30 MHz Riometer Events (Great Whale River)	6/65 - 2/67

D. Geomagnetic and Magnetospheric Phenomena

D.1a	Geomagnetic Indices Ci, Ks, Kn, Km, Cp, Kp, Ap, aa, Selected Days (aa first published 1/74; Ks, Kn, Km first published 12/75; Ci discontinued 8/75)	7/57 - present
D.1b	27-day Chart of Kp for Year	7/57 - present
D.1ba	27-day Chart of Kp Indices	7/57 - present
D.1c	27-day Chart of C9 for Year	7/57 - present
D.1d	Principal Magnetic Storms	7/66 - present
D.1e	Reduced Magnetograms	1/67 - present
D.1f	Sudden Commencements and Solar Flare Effects	1/66 - present
D.1g	Equatorial Indices Dst	5/73 - present
D.1h	Geomagnetic Substorm Log (Boulder)	3/78 - present

F. Cosmic Rays

F.1a	Cosmic Ray Daily Averages Neutron Monitors (Deep River - graph of hourly values, daily averages begin 11/65)	1/59 - present
F.1b	Cosmic Ray Daily Averages Neutron Monitors (Climax) Daily Averages and Graph of hourly values	9/60 - 3/72 12/74 - present
F.1c	Cosmic Ray Daily Averages Neutron Monitors (Dallas)	1/64 - 3/74
F.1d	Cosmic Ray Daily Averages Neutron Monitors (Churchill)	5/64 - 6/72
F.1e	Cosmic Ray Daily Averages Neutron Monitors (Alert) Graph of hourly values (Alert)	3/74 - present 7/66 - present
F.1f	Cosmic Ray Daily Averages Neutron Monitors (Calgary - also graph of hourly values)	1/71 - present
F.1g	Cosmic Ray Daily Averages Neutron Monitors (Sulphur Mountain - also graph of hourly values)	1/71 - present
F.1h	Cosmic Ray Daily Averages Neutron Monitors (Thule - also graph of hourly values)	4/73 - present
F.1i	Cosmic Ray Daily Averages Neutron Monitors (Tokyo - also graph of hourly values)	12/73 - present
F.1j	Cosmic Ray Daily Averages Neutron Monitors (Kiel - also graph of hourly values)	12/73 - present
F.1k	Cosmic Ray Daily Averages Neutron Monitors (Kula - also graph of hourly values)	5/77 - present

H. Miscellaneous

H.60	Alert and Special World Interval Decisions (IUWDS Geophysical Alerts)	7/57 - present
H.61	International Geophysical Calendar	1/62 - 12/62
H.62	Abbreviated Calendar Record	12/68 - present
H.63	Retrospective World Intervals	1/66 - 12/67

XIII. Note on INDEXES for UAG-23 and UAG-23A

If anyone feels corrections or additions should be made to the indexes for UAG-23 and UAG-23A published in INAG-29, please feel free to communicate them to your Chairman. Only with your assistance can we improve the index.